Received: 31 January 2020 | Revised: 31 August 2020 | Accepted: 16 October 2020

DOI: 10.1002/ese3.850

RESEARCH ARTICLE

Energy Science & Engineering
Open Access

Exergoeconomic analysis of a pumped heat electricity storage system based on a Joule/Brayton cycle

Axel Dietrich[1,2] | **Frank Dammel**[1,2] | **Peter Stephan**[1,2]

[1]Institute for Technical Thermodynamics, Technische Universität Darmstadt, Darmstadt, Germany

[2]Darmstadt Graduate School of Excellence Energy Science and Engineering, Technische Universität Darmstadt, Darmstadt, Germany

Correspondence
Frank Dammel, Institute for Technical Thermodynamics, Technische Universität Darmstadt, Darmstadt, Germany.
Email: dammel@ttd.tu-darmstadt.de

Funding information
Fritz and Margot Faudi-Foundation, TU Darmstadt, Grant/Award Number: Projekt 90; Deutsche Forschungsgemeinschaft, Darmstadt Graduate School of Excellence Energy Science and Engineering, Grant/Award Number: GSC 1070

Abstract

Storing electrical energy in the form of thermal energy, pumped heat electricity storage (PHES) systems are a location-independent alternative to established storage technologies. Detailed analyses, considering the transient operation of PHES systems based on commercially available or state-of-the-art technology, are currently not publicly accessible. In this work, numerical models that enable a transient simulation of PHES systems are developed using the process simulation software EBSILON® *Professional*. A PHES system based on a Joule/Brayton cycle is designed, considering commercially available and state-of-the-art components. Employing the developed models and an exergoeconomic analysis, the transient operation of the PHES system is simulated and evaluated. The analyzed PHES system reaches a round-trip efficiency of 42.9%. The exergoeconomic analysis shows that PHES systems have higher power-specific costs than established storage technologies. They can currently not be economically operated at the day-ahead market for Germany and Austria, which is predominantly resulting from high purchased equipment costs. However, PHES systems have the advantage of being location-independent.

KEYWORDS

electrical energy storage, exergoeconomic analysis, exergy analysis, PHES, pumped heat electricity storage

1 | INTRODUCTION

The share of renewable energy sources in the German gross electrical energy production was rising from 3.6% in 1990 up to 40.2% in 2019.[1] Extrapolating the trend shown in Figure 1, higher shares of renewable energy sources can be expected in the future. Adopted in July 2016, the newest version of the *Act on the Development of Renewable Energy Sources* (*Gesetz für den Ausbau Erneuerbarer Energien, EEG 2016*) targets to rise the share of renewable energy sources in gross electrical energy consumption to 40% in 2025, 55% in 2035, and 80% in 2050.[2] The higher the share of renewables, the stronger is the impact of the volatility of renewable energy sources on the production of electrical energy. More and more frequently, this results in a mismatch between the electrical energy supply and its demand. To maintain stability in the grid, supply and demand of electrical energy have to be balanced, because the grid itself cannot store electrical energy. Up to a certain degree, balancing of supply and demand can be achieved by flexible operation of power plants and load balancing. However, to reach the targets of the *EEG 2016*, medium- to large-scale storage systems for electrical energy are required.

Electrochemical accumulators have limitations in cyclic stability and require relatively large amounts of rare

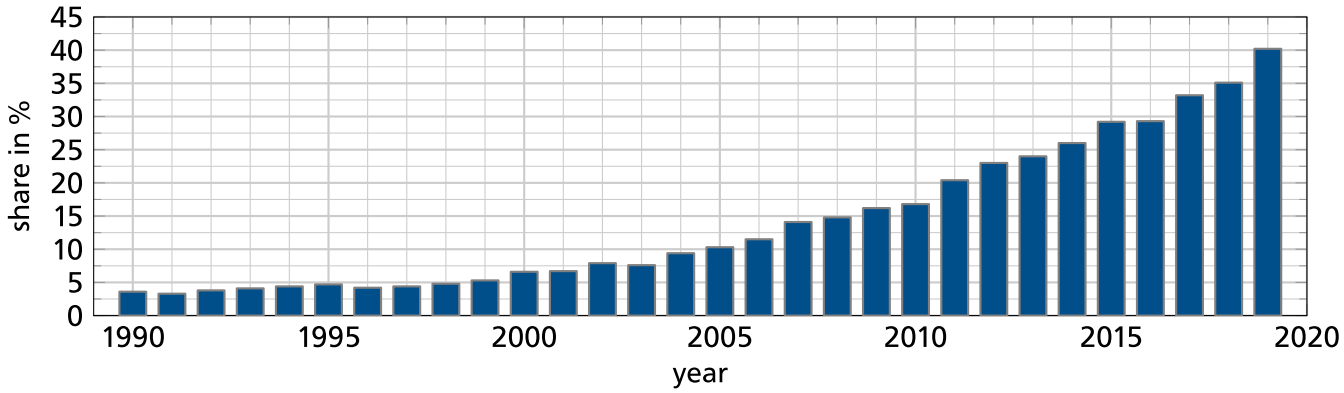

FIGURE 1 Share of renewable energy sources in the German gross electrical energy production [1]

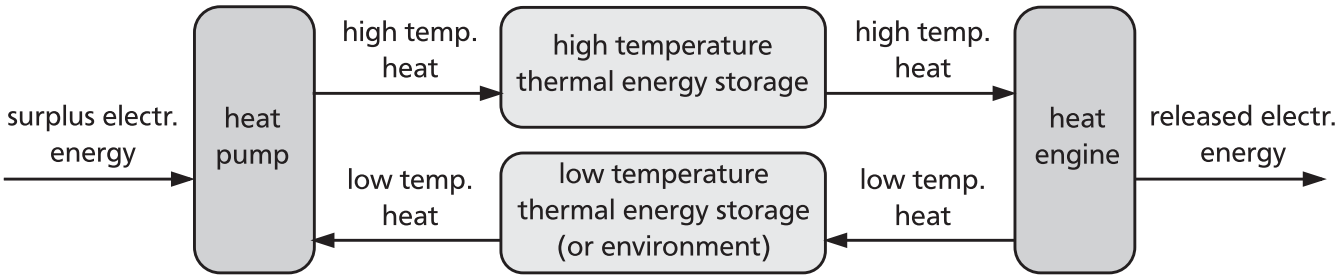

FIGURE 2 Common setup of a PHES system (boxes), including energy flows (arrows) [24]

elements, which is a disadvantage when used for large-scale storage of electrical energy. Nonchemical storage systems such as pumped hydro storage and compressed air energy storage can provide sufficient storage capacity but require special geological and geographical conditions[3] which limits their applicability for large-scale storage of electrical energy. A location-independent alternative is the relatively new technology known as pumped heat electricity storage (PHES) system which stores electrical energy via the detour of thermal energy in thermal energy storage (TES) subsystems.

Referring to the most common setup (Figure 2), PHES systems consist of the four subsystems heat pump, heat engine, high-temperature TES, and low-temperature TES. For most PHES systems, the high- and low-temperature TES subsystems comprise a single storage module, each. Nevertheless, different storage module numbers are possible. Simple setups do not contain a low-temperature TES; the environment is employed as low-temperature heat sink and heat source instead.

PHES systems can be operated to stabilize the electrical grid by acting either as consumer or as supplier. In times of high supply and low demand, the heat pump uses surplus electrical energy to pump heat taken from the low-temperature TES (or from the environment) to a higher temperature level. This high-temperature heat is forwarded to the high-temperature TES, where it is stored as thermal energy until the demand for electrical energy exceeds its supply. At those times the TES supplies heat to the heat engine which converts the thermal energy back into electrical energy. The low-temperature heat released by the heat engine is absorbed by the low-temperature TES (or by the environment).

Because they accomplish the energy storage between heat pump (charging) and heat engine (discharging) operation, TES systems are essential components of PHES systems (Figure 2). Latent heat TES systems reach a volume-specific energy density between 50 and 150 kWh m^{-3}[4] at minimum temperature differences within the TES. Sensible heat TES systems are characterized by a lower volume-specific energy density between 20 and 100 kWh m^{-3}[4] depending on temperature differences within the TES. However, sensible heat TES systems belong to the most developed storage technologies[4] are more established[4] and generate lower costs[5] than latent heat TES systems. Consequently, this work focuses on sensible heat TES systems. To minimize exergy destruction due to heat transfer, temperature differences between TES material and the working fluid of heat pump and heat engine are to be kept small. As a result, only PHES systems based on Joule/Brayton cycles are considered. In the following, they will be referred to as Joule cycles.

This paper presents a synopsis of [6] in which a more detailed essay of various approaches, models, and results can be found.

TABLE 1 Overview of research activities in the field of PHES systems based on Joule cycles

Group (company)	Working fluid	Thermal energy storage	Additional information, system and analysis shortcomings
Desrues, Ruer et al (SAIPEM-SA),[15,41], 2010	Argon	Two sensible TESs, refractory material (solid media), $T_{max} = 1000°C$, $T_{min} = -70°C$	Transient simulation with MATLAB and compiled C-code, compressor pressure ratio approximately 2, $E_{el,out} = 600$ MWh, $E_{el,in} = 900$ MWh, round-trip efficiency 66.7%, compressors, and TES subsystems for high storage temperatures commercially not available
Ni, Caram,[42], 2015	Argon	Usage of configuration presented by Desrues and Ruer	Transient simulation described with exponential matrix solution techniques, compressor pressure ratio considered between 2 and 5, round-trip efficiency between 60% and 100%, depending on chosen parameters, components for high storage temperatures are commercially not available
Howes (Isentropic),[43-45], 2012	Prototype: air, large-scale machine: argon	Two sensible packed bed TESs: particulate granite, $T_{max} = 500°C$, $T_{min} = -166°C$	Only performance extrapolation for hypothetical machine presented, $P = 2$MW, COP = 2.19, round-trip efficiency 72%, high efficiencies of the envisioned reciprocating compressor and expander are currently not state-of-the-art
McTigue et al,[46], 2015	Argon (utilization of large-scale machine invented by Howes)	Two sensible packed bed TESs: $T_{max} = 500°C$, $T_{min} = -166°C$	Simulation in quasi–steady state, optimization based on stochastic algorithms, round-trip efficiency between 50% and 70%, depending on the compression and expansion efficiencies
White et al,[47], 2013	Argon (utilization of PHES concepts invented by Howes and Desrues)	Utilization of storage concepts invented by Howes and Desrues	Simplified analytical analysis omitting transient effects in order to identify trends of efficiencies and losses, round-trip efficiencies up to 90%
Morandin et al,[48], 2011	Air	Two pairs of direct TESs for sensible heat storage: molten salt ($350°C < T < 700°C$) and synthetic oil ($100°C < T < 250°C$)	Preliminary performance estimation yields round-trip efficiency of 55%, high isentropic turbomachinery efficiency of 0.9 assumed
Laughlin,[49], 2017	Argon	Two pairs of direct TES for sensible heat storage: molten salt ($27°C < T < 550°C$) and hydrocarbon liquid ($-93°C < T < 222°C$)	Analytical analysis omitting transient effects yields round-trip efficiency of up to 72%, large TES temperature differences, high isentropic turbomachinery efficiency for compressor (0.91) and turbine (0.93)

2 | STATE OF THE ART OF HIGH-CAPACITY STORAGE SYSTEMS FOR ELECTRICAL ENERGY

PHES systems, as means to stabilize the electrical grid in periods of mismatch between electricity supply and demand, have to compete commercially with other high-capacity storage systems, namely pumped hydro storage systems and compressed air energy storage systems.

2.1 | Pumped hydro storage systems

Pumped hydro storage systems store electrical energy in the form of potential energy which results in negligible self-discharge and almost unlimited storage durations. At specific investment costs between 470 and 2170 € $(kW)^{-1}$, the round-trip efficiencies reach high values of 70% to 80%.[7,8] In contrast to PHES systems, pumped hydro storage systems demand for suitable topological conditions and seal large areas with their basins.[8]

2.2 | Compressed air energy storage systems

Compressed air energy storage (CAES) systems use electrical energy to power high-temperature air compressors in order to store pressurized air in underground caverns. To prevent the turbines from freezing during discharge, the compressed air has to be heated before expanding in turbine-generator sets that generate electrical energy. The necessary heat can be supplied by combustion of natural gas. Two such CAES systems are currently in operation. The system in Huntorf (Germany) has a storage-output capacity of 580 MWh_{el}[8] and reaches a round-trip efficiency of 46%.[9] Due to internal heat recovery during discharge, the system in McIntosh (USA) reaches a round-trip efficiency of 54%[9] having a storage-output capacity of 2860 MWh_{el}.[8]

In contrast to combusting natural gas, adiabatic CAES systems employ a thermal energy storage to store the heat released by the compressed air before it enters the underground cavern. During discharge, the stored heat is transferred back to the compressed air before it enters the turbine. Adiabatic CAES systems are subject to current research. With respect to working principle and required components, they have large similarities to PHES systems.

The project ADELE, led by the German Aerospace Center (DLR), was engaged in concept development and construction of a large-scale prototype of an adiabatic CAES system.[10-12] The development of suitable turbomachinery and TES subsystems issued the biggest challenge. High-temperature compressors are not state of the art yet, and they have to be developed.[12] Preliminary design calculations resulted in round-trip efficiencies of up to 70%.[12]

2.3 | Pumped heat electricity storage systems

The first concept of storing electrical energy via the detour of thermal energy dates back to as early as 1924. Marguerre [13] introduced a system consisting of two TESs filled with wet steam.

Steinmann[14] presented an extensive review of concepts for bulk energy storage. Basic concepts and current developments of PHES systems and related technology are summarized.

Considering current theoretical and experimental research activities, concepts of PHES systems based on Joule cycles are briefly summarized in Table 1. System and analysis shortcomings are also listed, from which the research objectives of this work are deduced in Section 3. A more detailed description of these studies can be found in [6].

3 | RESEARCH OBJECTIVES

Objective 1 To develop numerical models that enable a transient simulation and analysis of PHES systems based on Joule cycles.

Almost all publications about PHES systems present efficiency estimations and performance extrapolations, whereas steady-state and transient simulations of PHES systems are rare (Table 1). Especially, a detailed analysis of the transient system operation is mandatory to accurately evaluate the performance of storage systems in general and PHES systems in particular. The lack of transient analyses constitutes a research gap from which the first objective of this work is deduced. The transient analyses available in literature by Desrues et al[15] and Wang et al[16] do not fulfill the Objectives 2 and 3.

Objective 2 To evaluate the round-trip efficiency and exergetic performance of PHES systems based on commercially procurable and state-of-the-art technology.

The majority of performance estimations and simulations of PHES systems is based on efficiencies, temperatures, or temperature and pressure ranges that cannot be realized by employing state-of-the-art technology of individual system components. In some concepts, entire components are far from technical realization (Table 1). Evaluations and comparisons of PHES systems built of commercially procurable components at best, but at least based on state-of-the-art technology, are currently not available. Thus, an adequate mathematical model has to be established and numerical simulations have to be performed. Based on the numerical simulations (Objective 1) the system design yielding the highest round-trip efficiency has to be identified. The subsystem performance is also evaluated by means of an exergy analysis.

Objective 3 To evaluate the exergoeconomic performance of PHES systems based on commercially procurable and state-of-the-art technology.

The exergetic performance analysis (Objective 2) is extended to an exergoeconomic analysis of the PHES systems. Thereby, additional information is gained, allowing a cost estimation in comparison with alternative storage systems.

4 | PHES SYSTEM DESIGN

To achieve high round-trip efficiencies for PHES systems based on Joule cycles, five design constraints are deduced from the studies published in literature.

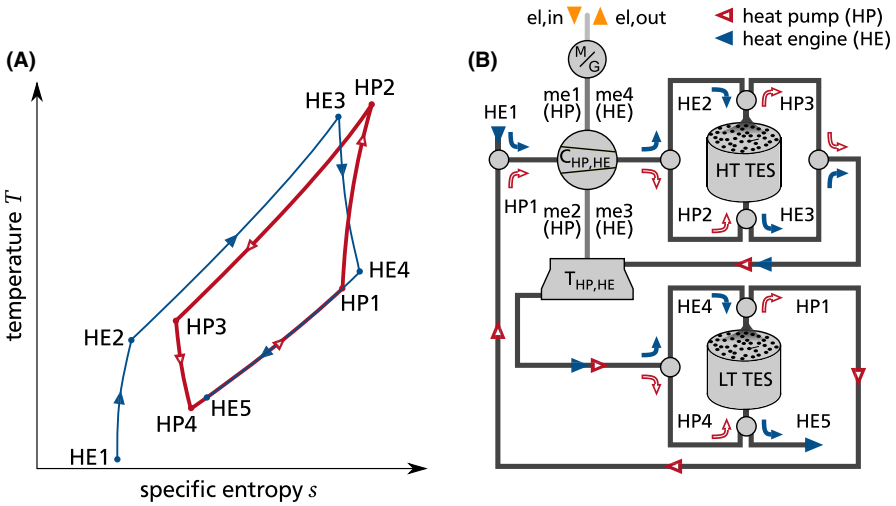

FIGURE 3 A, *T,s* diagram and B, schematic of the designed PHES system. The red arrows illustrate the path of the working fluid during heat pump operation, and the blue arrows illustrate the path of the working fluid during heat engine operation

1. If available, established technology should be employed in order to reduce technological risks.
2. The PHES system layout should be simple, limiting the amount of components to the essentially necessary required for an exergy efficient and cost-efficient operation.
3. Entropy rejection to the environment should be realized at small temperature and small pressure differences in order to minimize the associated exergy loss and exergy destruction.
4. The PHES system should be combined with a high- and a low- temperature TES instead of just one TES. This reduces the amount of heat exchanged with the environment and associated exergy losses.
5. Regenerative heat transfer does not improve the efficiency of PHES systems based on Joule cycles and is therefore not implemented. Due to the utilization of two TES subsystems, the low-temperature heat provided by the heat engine is already exploited. Moreover, steady-state design calculations indicated a reduction of round-trip efficiency, if regenerative heat transfer is implemented in PHES systems based on Joule cycles.

TABLE 2 Explanation of the changes of state for the PHES system based on the Joule cycles depicted in Figure 3

Change of state	Explanation
HP1-HP2	Compression ($p_{HP1} = p_{env}$)
HP2-HP3	Heat rejection to high-temperature TES
HP3-HP4	Expansion
HP4-HP1	Heat absorption from low-temperature TES
HE1-HE2	Air intake form the environment ($p_{HE1} = p_{env}$, $T_{HE1} = T_{env}$) and compression
HE2-HE3	Heat absorption from high-temperature TES
HE3-HE4	Expansion
HE4-HE5	Heat rejection to low-temperature TES and air output to the environment ($p_{HE5} = p_{env}$)

Considering these constraints, a PHES system based on the working fluid air is designed.[6] The corresponding *T,s* diagram with the thermodynamic cycles and a description of the changes of state are provided in Figure 3A and Table 2, respectively. Air was selected as working fluid in order to reject the generated entropy through a heat engine which is open to the environment. Thereby, the heat engine of the PHES system does not need to be equipped with an environmentally cooled condenser, which in turn reduces exergy destruction due to a vanishing condenser pressure drop. Also, costs for the condenser and the working fluid are saved.

A schematic of the PHES system is depicted in Figure 3B. Heat pump and heat engine share a single turbine-compressor shaft. The working fluid passes the TES subsystems in opposite directions during heat pump and heat engine operation in order to minimize exergy destruction and to reach the desired outlet temperatures. According to currently available technology, the efficiencies of motor and generator as well as the isentropic efficiencies of the turbomachinery are listed in Table 3. All efficiencies are given for the design point which defines the optimal operating point of the components.

As motivated at the end of Section 1, sensible heat TES subsystems are integrated into a PHES system based on Joule cycles. For a reasonable heat transfer between working fluid and TES material, a packed bed arrangement is chosen. Based on a study by Rundel[17] examining the long-term thermal and mechanical stability of packed beds, basalt chips without quartz content are selected as TES material. This

TABLE 3 Summary of component efficiencies of the Joule cycle based PHES system at the design point

Component	Efficiency	References
Motor	0.96 (energetic)	[23]
Generator	0.96 (energetic)	[23]
Compressor	0.85 (isentropic)	[23,50]
Turbine	0.90 (isentropic)	[23,50]

Specific heat capacity $c_{p,Pa}$ in J (kg K)$^{-1}$	Thermal conductivity λ_{Pa} in W (m K)$^{-1}$	Density ρ_{Pa} in kg/m^3	Void fraction ε (by volume)
1004	1.7	2950	0.40

Note: value for void fraction taken from [51]

TABLE 4 Material properties (averaged in the relevant temperature range) [5] of basalt chips without quartz content used as TES material in the form of a packed bed

material performed best among all tested materials; without any degradation, it withstood 7000 charging and discharging cycles with inlet temperatures of 600 and 24°C, respectively. Relevant material properties of basalt chips without quartz content are summarized in Table 4. Heat losses to the environment are neglected because proper insulation of the cylindrical TES container is provided. Panels of microporous insulation material ($\lambda|_{\Delta T=600K} = 0.04 W(\mathrm{mK})^{-1}$[18]) having a thicknesses of 0.5 m at the side and 2.0 m at the top and bottom walls of the TES provide sufficient insulation.[19]

Krüger et al[20] identified potential economic and operational feasibility for small-scale electrical energy storage systems with a charge/discharge power of 10 to 30 MW_{el}, charge/discharge times of 4.0 to 6.5 hours, and capacities in the order of 50 to 150 MWh_{el}. In this work, PHES systems classified at the lower boundaries of the aforementioned ranges are considered.

The design parameters of the PHES system analyzed in this work are summarized in Table 5. Data published by the ADELE project[20-22] are used as a reference for currently available technology in order to determine the maximum temperature $T_{max,HP}$ and the maximum mass flow $\dot{M}_{max}$. Influenced by the maximum mass flow and based on the results of Krüger et al,[20] who investigated the economic feasibility of small-scale adiabatic CAES systems, the electrical input power consumed by the heat pump $P_{el,in}$ is set. Taking characteristic charging and discharging durations into consideration, which are derived in Section 6.2 and summarized in Table 6, yields the electrical energy consumed by the PHES system $E_{el,in}$ during heat pump operation.

Having selected the maximum temperature of the working fluid in the heat pump $T_{max,HP}$ and considering a constant exergy content to be stored by the PHES system, the maximum pressure of the working fluid in the heat engine $p_{max,HE}$ influences the round-trip efficiency of the PHES system. The higher the maximum pressure, the higher the exergy destruction becomes in the turbomachinery. In turn, the temperature difference and, hence, the exergy destruction experienced by the working fluid when passing through the TES systems decreases with increasing maximum pressure. These reverse effects indicate the existence of an optimal maximum pressure which was determined in [6].

The size of the TES systems is a result of the electrical energy $E_{el,in}$ to store. Diameter d_R and height l_R of the packed bed in the cylindrical TES container are equal in order to minimize the outer surface area of the container. The diameter d_{Pa} of the packed bed particles is chosen as large as possible in order to reduce pressure drop and as small as necessary to avoid temperature gradients within the particles.

5 | SYSTEM MODELING

The process simulation software EBSILON® *Professional*[23] is used as platform to model and simulate PHES systems. All components of the thermodynamic cycles are simulated in quasi–steady state whereas a transient simulation is used for the TES subsystems.

5.1 | Thermodynamic cycles

To model and simulate the thermodynamic cycles of heat pump and heat engine, the built-in components of EBSILON®

TABLE 5 Summary of design parameters of the Joule cycle based PHES system analyzed in this work

Design parameters	Design values
Heat pump	
Maximum temperature in °C	600
Maximum working fluid mass flow in kg/s	110
Power input $P_{el,in}$ in MW	12.6
Electrical energy input $E_{el,in}$ in MWh	50.4
Heat engine	
Maximum pressure $p_{max,HE}$ in bar	2.549
High- and low-temperature TES (each)	
Mass (of particles) in t	3650
Diameter of particle bed d_R in m	13.80
Height of particle bed l_R in m	13.80
Particle diameter d_{Pa} in mm	30

TABLE 6 Specification of the characteristic operation scenario used for the exergoeconomic analysis

Operation mode	Start time in h	End time in h	Duration in h	Averaged electricity price
Heat pump (charging)	01:00	05:00	4	19.66 € $(MWh)^{-1}$
Idle after heat pump	05:00	17:00	12	—
Heat engine (discharging)	17:00	21:00	4	38.42 € $(MWh)^{-1}$
Idle after heat engine	21:00	01:00	4	—

Professional are used. The components' default mathematical models, equations, and correlation coefficients were used, which are documented with the software.[23] First, the design point of the thermodynamic cycle was modeled and simulated. Afterward, the off-design performance, the operation outside of the design point, was simulated. All off-design simulations are based on the default component-specific off-design performance characteristics documented with the software.[23]

5.2 | Sensible heat thermal energy storage subsystems

EBSILON® *Professional* provides a basic storage model for a sensible heat thermal energy storage subsystem.[1] The model consists of a single pipe conducting the working fluid encased by a cylindrical shell containing the storage material (Figure 4). The dimensions of pipe and shell can be adapted but the basic topology cannot be changed. The solver is based on a cylindrically symmetrical finite differences approach using the implicit Crank-Nicolson method on a rectangular grid.

The adaptions made on the basic storage model to simulate a sensible heat TES in the form of a massive block traversed by multiple pipes are described in.[24] To enhance heat transfer between working fluid and storage material, the storage material is integrated in the form of a packed bed instead of a massive block.

Ismail and Stuginsky[25] present an extensive overview and comparison of modeling approaches for packed bed TES systems. More condensed reviews are provided by Hänchen et al[26] and Gil et al.[27] For integration into the framework of the EBSILON® *Professional* basic storage model, a one-dimensional, two-phase approach is developed, which is similar to the one by Hänchen et al.[26] The developed modeling approach is based on the following assumptions:

- uniformly packed bed,
- turbulent flow conditions of the working fluid, which are homogeneous when temporally averaged over the flow cross section,
- the thermal energy storage capacity of the working fluid can be neglected,
- heat losses to the environment can be neglected,
- temperature inhomogeneities within particles can be neglected.

The modeling approach for a packed bed sensible heat TES is depicted in Figure 5. A detailed description of the modeling approach and its successful validation through comparisons with experimental data and simulation results is presented in [6]

6 | METHODOLOGY AND ANALYSIS PROCEDURES

6.1 | Exergoeconomic analysis

Based on simulation results or real process data, an exergy analysis provides the exergy distribution among the components of a system. Exergy is the maximum amount of work that can be conducted by a system, if the system is reversibly brought into equilibrium with its environment. Detailed introductions, several definitions, and derivations of the concept of exergy can be found in.[28-30]

Adapted to the operation scenario analyzed, component costs and costs for input quantities are provided by an economic analysis. A detailed description of the procedures employed to determine costs can be found in [6]

An exergoeconomic analysis combines the results of an exergy analysis and an economic analysis (Figure 6) in order to allocate costs among the components of a system. Costs C are assigned to exergy E via exergy costing [29,31]

$$C = c\,E, \tag{1}$$

introducing the specific costs per exergy c, which can be determined by cost balances. Cost balances are compiled for each system component (Equations 2 and 3) equating the costs entering the component and the costs generated in the component with the cost leaving the component.

$$\sum_{j=1}^{j_{max}} C_{\mathrm{in},j} + Z^{\mathrm{OP}} = \sum_{k=1}^{k_{max}} C_{\mathrm{out},k} \tag{2}$$

$$\sum_{j=1}^{j_{max}} (c_{\text{in},j} \cdot E_{\text{in},j}) + Z^{\text{OP}} = \sum_{k=1}^{k_{max}} (c_{\text{out},k} \cdot E_{\text{out},k}). \quad (3)$$

An exergoeconomic analysis accounts for energy conversion efficiency, physical limits of energy conversion, and financial costs of energy conversion. The development of exergy and exergoeconomic analyses is summarized in detail by Tsatsaronis.[31] An extensive review of the same matter is presented by Sciubba and Wall.[32]

6.2 | Characteristic operation scenario

In order to determine the time of the day at which a PHES system should be charged and discharged, the European market for electrical energy[6] is analyzed. The day-ahead market for Germany and Austria shows a high predictability regarding daily repetitiveness of the electricity price distribution.[33] Based on market principles, hourly averaged prices for electrical energy at the day-ahead market for the year 2016 are used as indicator for supply and demand (Figure 7). For each day of the year, the continuous 4-hour time periods with the lowest and highest average electricity price between 23:00 hours of the previous day and 24:00 hours are determined. Averaging the electricity prices of all determined time periods over the entire year results in average market prices of 19.66 € $(\text{MWh})^{-1}$ = 1.966ct $(\text{kWh})^{-1}$ during the heat pump operation and 38.42 € $(\text{MWh})^{-1}$ = 3.842ct $(\text{kWh})^{-1}$ during the heat engine operation of the PHES system. A summary of the deduced characteristic operation scenario used for the exergoeconomic analysis is provided in Table 6. The PHES system shall perform a complete operation period once within 24 hours.

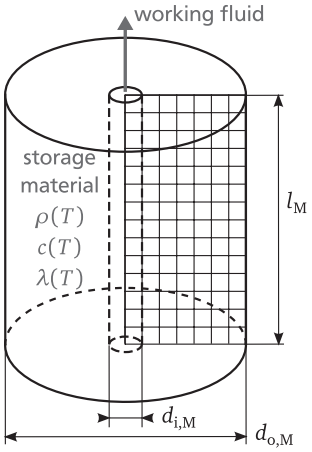

FIGURE 4 Layout of the sensible heat TES model implemented in EBSILON®*Professional*. Density ρ, specific heat capacity c, and thermal conductivity λ of the storage material can be defined as constants or variables, linearly depending on temperature

6.3 | Cyclic steady-state analysis

The transient operation of the PHES system is simulated. Due to varying storage inlet and outlet conditions, the charge states of the TES subsystems influence the operation of the other PHES subsystems and vice versa. The individual charge state is characterized by a specific distribution of internal energy and temperature within the storage material.

A meaningful and reproducible analysis has to be independent of charge states. The simulation of consecutive operation periods of the PHES system according to the characteristic operation scenario eventually converges into the cyclic steady state. This holds true for any arbitrary initial temperature distribution within the TES systems as long as the temperatures are compatible with the chosen heat pump/heat engine design. Operation periods in cyclic steady state have the following characteristics:

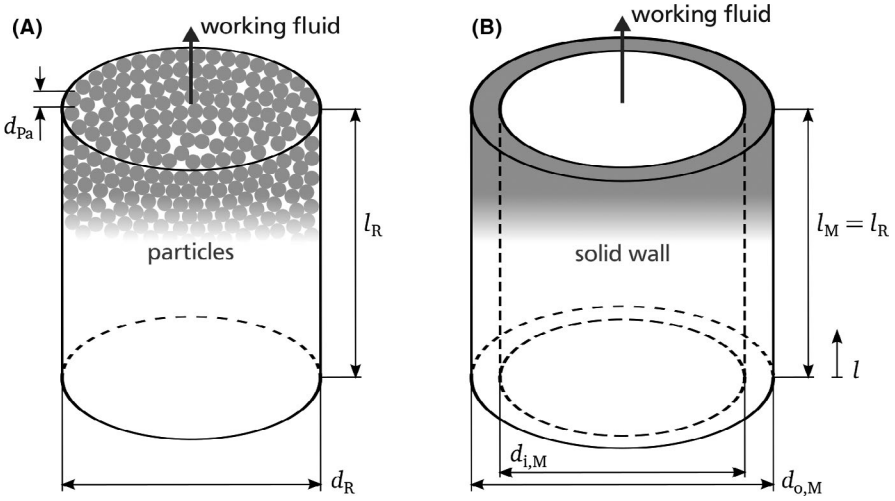

FIGURE 5 A, Topologies of the packed bed sensible heat TES and B, its model implemented in EBSILON®*Professional*

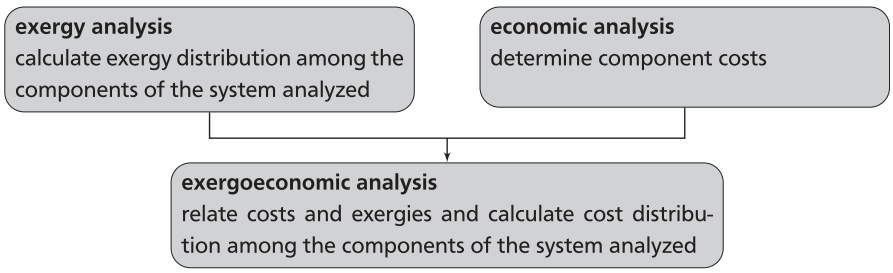

FIGURE 6 Basic principle of an exergoeconomic analysis

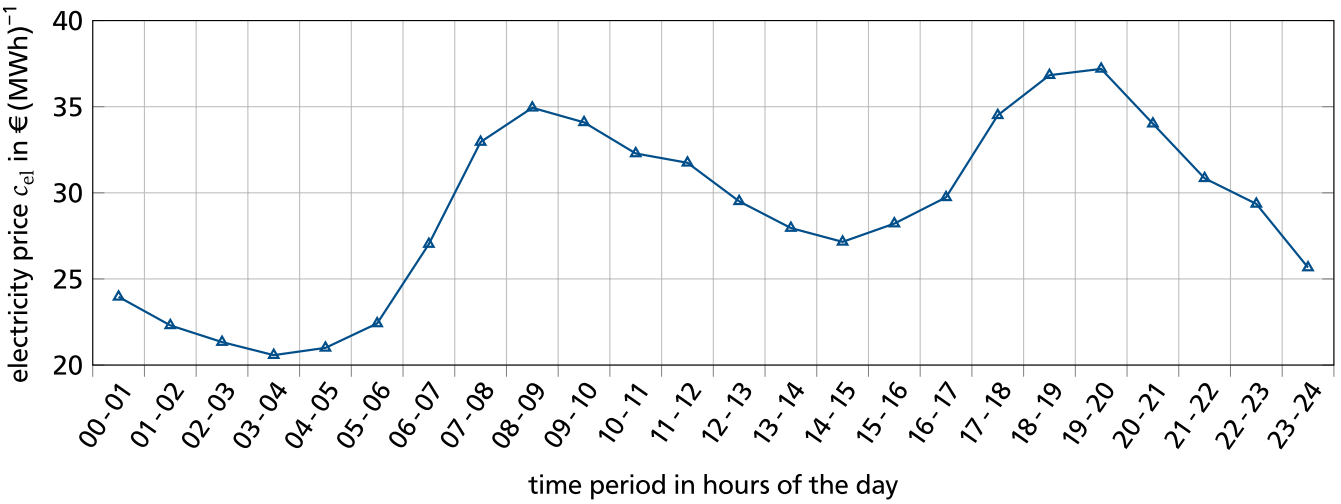

FIGURE 7 Hourly averaged prices for electrical energy at the day-ahead market for Germany and Austria in the year 2016 [33]

- the end of one period marks the beginning of the following period,
- all periods take the same time,
- each TES subsystem has identical charge states at the beginning and at the end of the operation period,
- the time-dependent course of the PHES operation is identical for all operation periods.

All exergoeconomic analyses in this work are based on the simulation results of a characteristic operation period in cyclic steady state.

7 | ANALYSIS AND RESULTS

7.1 | Exergy analysis

During operation, the components of the PHES systems exchange exergy flows $\dot{E}$ through the entering and exiting working fluid $\dot{M}$.

$$\dot{E} = \dot{M}((h - h_{env}) - T_{env}(s - s_{env})) \tag{4}$$

h_{ref} and s_{ref} denote the working fluid's enthalpy and entropy at environmental conditions, respectively:

$$T_{env} = 10\,^{\circ}\mathrm{C} \tag{5}$$

$$p_{env} = 1\ \mathrm{bar}. \tag{6}$$

The temperature of the environment is equal to the mean temperature in Germany in the years 2015 and 2016.[34,35] Based on the characteristic operation scenario (Section 6.2) evaluated in cyclic steady state (Section 6.3), the time-dependent exergy flows $\dot{E}$ processed by each component are integrated over the entire operation period. The resulting amounts of exergy E are then processed in the exergy and exergoeconomic analyses.

The inlet, outlet, and mean temperature distribution of the high- and low-temperature TES subsystems over time are depicted in Figure 8. The working fluid inlet temperature to the high-temperature TES stays constant during heat pump and heat engine operation. This is necessary in order to reach a stable cyclic steady-state operation. After remaining constant until approximately 2 hours of operation time, the working fluid outlet temperature of the high-temperature TES deviates in the direction of the inlet temperature. The inlet and outlet temperatures of the working fluid passing through the low-temperature TES adjust automatically to the operation conditions of the PHES system.

For the PHES system and its subsystems, Table 7 summarizes energetic and exergetic efficiencies, the underlying fuel and product definitions, as well as the exergy destruction integrated over the entire operation period of 24 hours. The

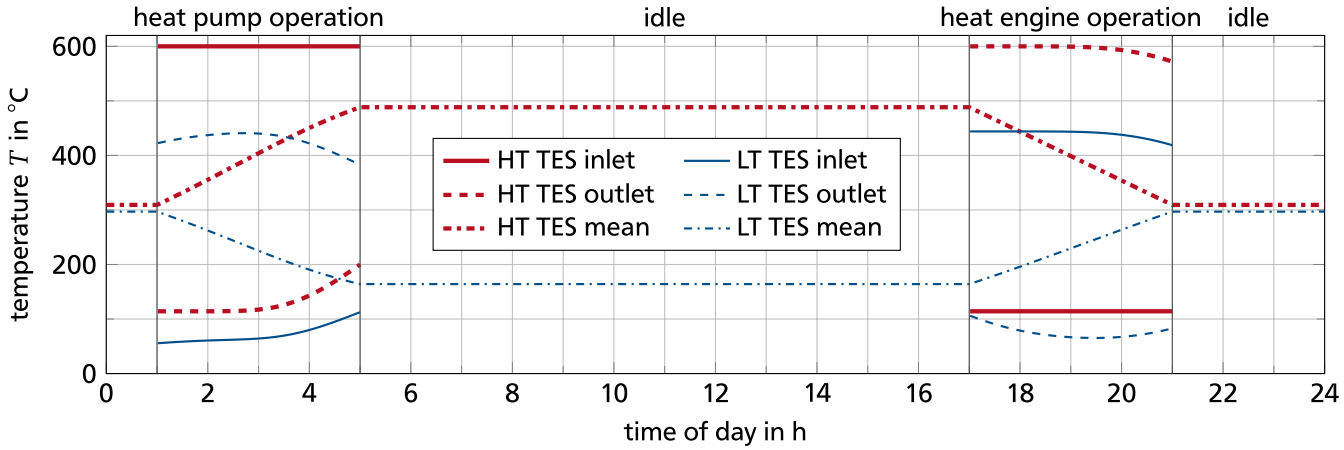

FIGURE 8 Time curves of inlet, outlet, and mean temperature of the high- and low-temperature TES

product of the heat pump and fuel of the TES are the energy/exergy released by the working fluid in the HT TES minus the energy/exergy received by the working fluid in the LT TES. The product of the TES and fuel of the heat engine are the energy/exergy received by the working fluid in the HT TES minus the energy/exergy released by the working fluid in the LT TES. Energetic and exergetic efficiencies are determined by

For the PHES system, the exergetic efficiency is equal to

$$\eta_{\text{en}} = \frac{\text{En}_{\text{product}}}{\text{En}_{\text{fuel}}}, \quad \eta_{\text{ex}} = \frac{E_{\text{product}}}{E_{\text{fuel}}}. \tag{7}$$

the energetic efficiency because both, fuel and product, are electrical energy which consists entirely of exergy.

The TES subsystems have the highest exergetic efficiencies, followed by heat pump and heat engine. The exergy destruction indicates the same trend. The relatively low exergy destruction of the TES subsystems is caused by two effects. First, the temperature difference between working fluid and storage material during charging and discharging is small compared with the temperature difference to the environment. Second, the thermal conductivity between the particles of the TES is small, which impairs the degradation of the temperature profile within the TES during the idle time.

The propagation of exergy through the PHES system is visualized in the Sankey diagram in Figure 9. For a complete overview of the PHES system performance, exergetic efficiencies are also listed. The Sankey diagram exemplifies that a multiple of the exergy entering and leaving the PHES system is stored in the TES subsystems. Furthermore, the propagation of exergy through the PHES system illustrates that the low-temperature TES is an important component. Without the low-temperature TES being present, the heat engine would release a substantial amount of exergy to the environment. This exergy would be missing during heat pump operation, approximately cutting the round-trip efficiency in half.

7.2 | Economic analysis

The economic analysis allocates costs to each component and each input quantity of the PHES system. Due to a scarcity of reliable, up-to-date data, market researches do not prove useful for determining purchased equipment costs. Consequently, the purchased equipment costs of most of the components employed in this work draw on cost correlations by Turton et al[36] and Towler et al.[37]

For the motor/generator set, a basic cost-scaling approach[29,36] is employed to determine the purchased equipment costs, drawing on performance and cost data by Balli et al.[38] The costs of the TES subsystem include costs for the storage material basalt chips of 200 € t^{-1}.[39]

The purchased equipment costs Z^{PEC}, annual component costs Z^{an}, and the component costs per operation period Z^{OP} are summarized in Table 8. All costs are projected to the reference year 2016 employing the Chemical Engineering Plant Cost Index[40] and converted to Euro.

Employing the annuity method,[29] the annual component costs Z^{an} result from leveling the purchased equipment costs over the entire projected operating time of $n^{\text{an}} = 20a$ under consideration of a compounded interest rate $i = 1.5\%$ and an annual operation and maintenance cost factor $\gamma = 1.5\%$

$$Z^{\text{an}} = \left(\frac{i(1+i)^{n^{\text{an}}}}{(1+i)^{n^{\text{an}}} - 1} + \gamma \right) Z^{\text{PEC}}. \tag{8}$$

Finally, dividing the annual component costs by the amount of operation cycles per year $N^{\text{an}} = 365$ yields the component costs per operation period Z^{OP}.

TABLE 7 Integrated exergy destruction, fuel and product definitions, and energetic and exergetic efficiencies for the subsystems and the entire PHES system

(Sub-)system	Fuel definition	Product definition	η_{en}	η_{ex}	E_D in MWh
HP	el,in	HP2 – HP3 – (HP1 – HP4)	0.935	0.804	9.87
TES	HP2 – HP3 – (HP1 – HP4)	HE3 – HE2 – (HE4 – HE5)	1.000	0.851	6.03
HE	HE3 – HE2 – (HE4 – HE5)	el,out	0.458	0.626	12.90
PHES	el,in	el,out	0.429	0.429	28.80

Note: The nomenclature of the components and attached fluid pipes, electrical leads, and mechanical shafts follows Figure 3B.

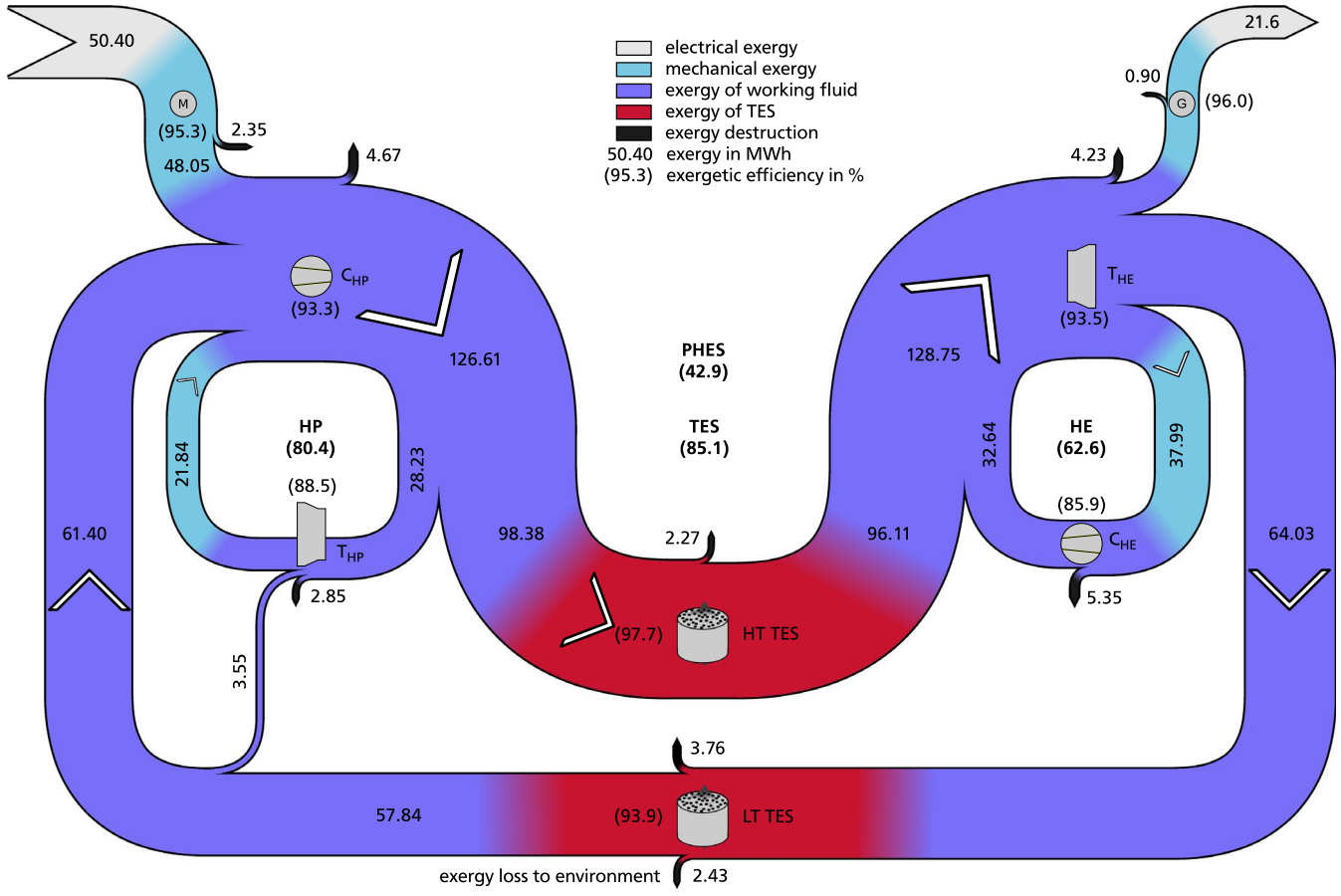

FIGURE 9 Sankey diagram visualizing the propagation of exergy through the PHES system

TABLE 8 Purchased equipment costs, annual costs, and costs per operation period for each component of the PHES system

Component	Z^{PEC} in k€	Z^{an} in k€	Z^{OP} in k€
Compressor	7362	539.2	1.477
Turbine	7570	554.4	1.519
Motor/generator	597	43.7	0.120
HT TES	1043	76.4	0.209
LT TES	1043	76.4	0.209

As input parameters to the exergoeconomic analysis, the component costs per operation period represent cost sources within each component. According to the chosen system design, heat pump and heat engine share compressor, turbine, and motor/generator. Therefore, half of the component costs per operation period of these components is assigned to the heat pump and the other half is assigned to the heat engine. The specific costs for electrical energy consumed by the heat pump amount to $c_{el,in}$ = 19.66 € $(MWh)^{-1}$, as determined in Section 6.2.

TABLE 9 Auxiliary equations and boundary conditions for the exergoeconomic analysis of the PHES system

Auxiliary equations	Description
$c_{HP2} = c_{HP3}$	Constant exergy-specific costs of working fluid passing the HT TES
$c_{HP3} = c_{HP4}$	Constant exergy-specific costs of working fluid passing the heat pump turbine
$c_{HE3} = c_{HE4}$	Constant exergy-specific costs of working fluid passing the heat engine turbine
$c_{me3} = c_{me4}$	Constant exergy-specific costs along the shaft of the heat engine
Boundary conditions	Description
$c_{HE1} = 0$	No costs attached to the air entering the heat engine
$c_{HE5} = 0$	No costs (or revenues) attached to the air leaving the heat engine
$c_{el,in} = 19.66$ € $(MWh)^{-1}$	Specific costs for electrical energy entering the heat engine (Section 6.2)

TABLE 10 Summary of variables characterizing the exergoeconomic performance of the PHES system and its subsystems

	E_F	E_P	C_F	C_P	c_F	c_P	η_{ex}	E_D	Z^{OP}
	in MWh		in €		in € $(MWh)^{-1}$		-	in MWh	in €
HP	50.40	40.53	991	2549	19.66	62.89	0.804	9.87	1558
TES	40.53	34.50	2549	2967	62.89	86.01	0.851	6.03	419
HE	34.50	21.60	2967	4525	86.01	209.51	0.626	12.90	1558
PHES	50.40	21.60	991	4525	19.66	209.51	0.429	28.80	3535

7.3 | Exergoeconomic analysis

The simulation results are based on the characteristic operation scenario (Section 6.2) evaluated in cyclic steady state. For each component, a cost balance is compiled (Equation 3) forming a linear system of equations for the entire PHES system. The auxiliary equations and boundary conditions necessary to solve the linear system of equations are listed in Table 9. An overview of the most important variables describing the exergoeconomic performance of the PHES system and its subsystems is given in Table 10. The fuel and product definitions presented in Table 7 apply. The absolute cost difference across each subsystem is equal to the sum of component costs per operation period for that subsystem.

The specific costs per exergy for fuel c_F and product c_F are derived by Equation 1. As heat pump and heat engine share the same components, the absolute cost differences across these subsystems are equal. Due to a higher exergy destruction at identical component costs, the heat engine has a slightly worse exergoeconomic performance than the heat pump. The TES subsystem has the best exergoeconomic performance among all subsystems, because it is subject to the smallest exergy destruction (caused by the highest exergetic efficiency) in combination with the smallest component costs per operation period.

$$C_F + Z^{OP} = C_P \tag{9}$$

The specific costs per exergy product c_P are a good indicator of exergoeconomic system performance; the lower these costs are, the better the performance is. Depending on the component costs per operation period, a favorable exergetic performance is not necessarily tied to a favorable exergoeconomic performance.

The propagation of absolute costs through the PHES system is visualized in the Sankey diagram in Figure 10. For a complete overview of the PHES system performance, exergy-specific costs are also listed. The Sankey diagram exemplifies that a multiple of the costs entering and leaving with the electrical energy is attached to the exergy propagating through the PHES system. During operation in cyclic steady state, these costs are not entering or leaving the PHES system.

The PHES system entails at least 36% higher investment costs per installed output power than the ADELE adiabatic CAES system or pumped hydro storage systems (Table 11). For the PHES system, the determined investment costs per installed output power are solely based on the purchased equipment costs (Section 7.2). If additional cost sources are

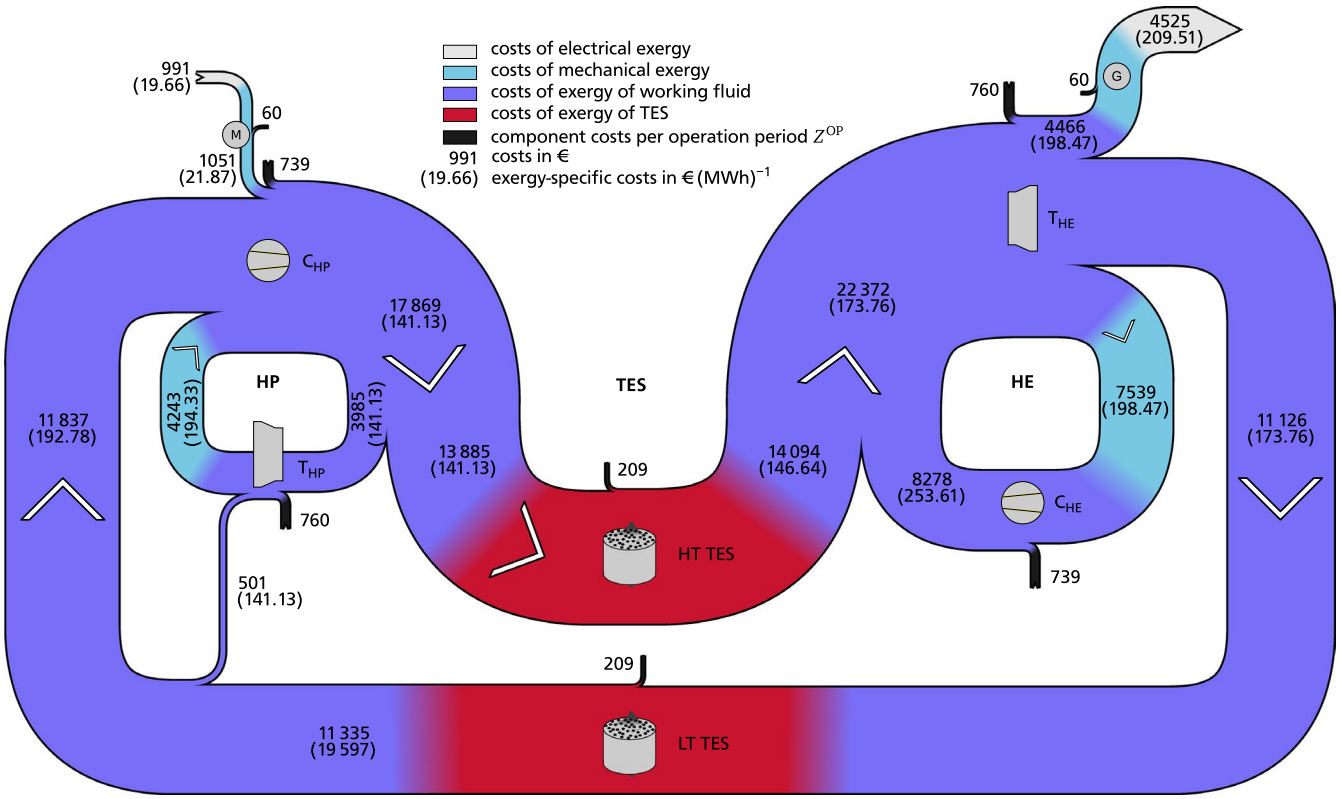

FIGURE 10 Sankey diagram visualizing the propagation of costs through the PHES system

TABLE 11 Comparison of the investment costs per installed output power for different electrical energy storage systems

Storage technology	Investment costs per installed output power in € $(kW_{el})^{-1}$	References
PHES system	3260	
ADELE adiabatic CAES	1500-2400	[12]
Pumped hydro storage	470-2170	[7]

considered, the difference to the other storage technologies will further increase.

Considering the economic conditions at the day-ahead market for Germany and Austria in the year 2016, the PHES system cannot be operated profitably. Based on the characteristic operation scenario (Section 6.2), the average market price during the heat engine operation amounts to 38.42 € $(MWh)^{-1}$ (Table 6). With specific prices for electrical energy supplied by the heat engine of 209.51 € $(MWh)^{-1}$, the attainable market price is exceeded by a factor of 5.45.

8 | SUMMARY AND OUTLOOK

In this work, numerical models that enable a transient simulation of PHES systems were created using the process simulation software EBSILON® *Professional*. Employing commercially available and state-of-the-art components, a PHES system based on Joule cycles was designed, simulated, and analyzed.

The PHES system reaches a round-trip efficiency of 42.9%, which is approximately half the efficiency reached by pumped hydro storage systems[7,8] and adiabatic CAES systems.[12] Compared to nonadiabatic CAES systems, which are currently in operation, the PHES system has an approximately 10 percentage points lower round-trip efficiency.

Predominantly resulting from high purchased equipment costs, the PHES system has higher power-specific costs than established technologies. Supplying electrical energy at costs that exceed acceptable market prices by more than a factor of five, PHES systems can currently not be economically operated at the day-ahead market for Germany and Austria. However, this is at least partly caused by current market conditions, which are unfavorable for the operation of electrical energy storage systems.

Considering the analysis results combined with the independence from geological and topological conditions, PHES systems are assessed as relevant technology to store electrical energy.[6,24] Being subject to ongoing research activities, PHES systems based on the Rankine cycles are going to be designed and analyzed. The exergoeconomic analyses of the Joule and Rankine cycles based PHES systems are going to be compared.

ACKNOWLEDGMENTS

This project was financially supported by the Fritz and Margot Faudi-Foundation, TU Darmstadt. Further financial support came from the DFG in the framework of the Excellence Initiative, Darmstadt Graduate School of Excellence Energy Science and Engineering (GSC 1070).

NOMENCLATURE

Latin letters (Unit)	Description
C (€)	costs
c (€ J^{-1})	exergy-specific costs
c (J (kg K)$^{-1}$)	specific heat capacity
d (m)	diameter
E (J)	exergy
En (J)	energy
h (J (kg)$^{-1}$)	specific enthalpy
i (-)	interest rate
l (m)	height
M (kg)	mass
N^{an} (-)	number of operation periods per year
n^{an} (a)	projected operating time
P (W)	power
p (Pa)	pressure
s (J (kg K)$^{-1}$)	specific entropy
T (°C)	temperature
Z^{an} (€)	component costs per year
Z^{OP} (€)	component costs per operation period
Z^{PEC} (€)	purchased equipment costs

Greek letters (Unit)	Description
γ (–)	annual operation and maintenance cost factor
ε (–)	volumetric void fraction of a packed bed
η (–)	efficiency
λ (W (m K)$^{-1}$)	thermal conductivity
ρ (kg/m^3)	density

Subscripts	Description
D	destruction
el	electrical
en	energetic
env	environment
ex	exergetic
F	fuel
i	inner
in	inlet
M	model of thermal energy storage module
max	maximum
min	minimum
o	outer
out	outlet
P	product
Pa	particle
R	real thermal energy storage module
sys	system

Abbreviations	Description
ADELE	German acronym for adiabatic compressed air energy storage (Adiabater Druckluftspeicher für die Elektrizitätsversorgung)
C	compressor
COP	coefficient of performance
CAES	compressed air energy storage
DLR	German Aerospace Center
G	generator
HE	heat engine
HP	heat pump
HT	high-temperature
LT	low-temperature
M	motor
PHES	pumped heat electricity storage
PEC	purchased equipment costs
T	turbine
TES	thermal energy storage

ORCID

Frank Dammel https://orcid.org/0000-0003-4021-8031
Peter Stephan https://orcid.org/0000-0003-1547-560X

ENDNOTE

[1] COMPONENT 119 (INDIRECT STORAGE).

REFERENCES

1. AG Energiebilanzen. Share of renewable energy sources in gross electrical energy production in Germany from 1990 to 2019, Statista - Statistik Portal. 2019.
2. Deutscher Bundestag, Gesetz zur Einführung von Ausschreibungen für Strom aus erneuerbaren Energien und zu weiteren Änderungen des Rechts der erneuerbaren Energien, EEG, Paragraph 1. 2016.
3. Thess A. Thermodynamic efficiency of pumped heat electricity storage. *Phys Rev Lett*. 2013;111(11):110602. https://doi.org/10.1103/PhysRevLett.111.110602
4. Laing D. Wärmespeichertechnologien für Energieeffizienz in Industrieanwendungen. In: *Energie Speicher Symposium*. Stuttgart; 2012.
5. Rundel PM, Meyer B, Meiller M, et al. *Speicher für die Energiewende, report*. Sulzbach-Rosenberg: Fraunhofer-Institut für Umwelt-, Sicherheits- und Energietechnik UMSICHT; 2013.
6. Dietrich A. *Assessment of Pumped Heat Electricity Storage Systems Through Exergoeconomic Analyses*. Ph.D. thesis. Darmstadt: Technische Universität Darmstadt; 2017. https://tuprints.ulb.tu-darmstadt.de/id/eprint/6752
7. Deane JP, Gallachóir BPÓ, McKeogh EJ. Techno-economic review of existing and new pumped hydro energy storage plant. *Renewab Sustain Energy Rev*. 2010;14(4):1293-1302. https://doi.org/10.1016/j.rser.2009.11.015
8. Neupert U, Euting T, Kretschmer T, Notthoff C, Ruhlig K, Weimert B. *Energiespeicher - Technische Grundlagen und*

Energiewirtschaftliches Potenzial. Stuttgart: Fraunhofer IRB Verlag. 2009.
9. Hartmann N, Vöhringer O, Kruck C, Eltrop L. Simulation and analysis of different adiabatic compressed air energy storage plant configurations. *Appl Energy*. 2012;93:541-548. https://doi.org/10.1016/j.apenergy.2011.12.007
10. Zunft S, Krüger M, Marquardt R, et al. Adiabate Druckluftspeicher für die Elektrizitätsversorgung. In: Beckmann M, Hurtado A (Eds.), *Kraftwerkstechnik - Sichere und nachhaltige Energieversorgung*, Vol. 3. Neuruppin: TK-Verlag; 2011:579-590.
11. Zunft S, Krüger M, Dreißigacker V, Mayer P-M, Niklasch C, Bertsch C. Adiabate Druckluftspeicher für die Elektrizitätsversorgung – der ADELE-Wärmespeicher. In: Beckmann M, Hurtado A (Eds.), *Kraftwerkstechnik - Sichere und nachhaltige Energieversorgung*, Vol. 4. Neuruppin: TK-Verlag; 2012:749-757.
12. Marquardt R, Moser P, Niklasch C, et al. Adiabate Druckluftspeicher für die Elektrizitätsversorgung – Status des Projektes ADELE-ING. In: Beckmann M, Hurtado A (Eds.), *Kraftwerkstechnik - Sichere und nachhaltige Energieversorgung*, Vol. 5. Neuruppin: TK-Verlag; 2013:803-819.
13. Marguerre F. Über ein neues Verfahren zur Aufspeicherung elektrischer Energie. *Mitteilungen der Vereinigung der Elektrizitätswerke*, 1924;354(55):27-35.
14. Steinmann W-D. Thermo-mechanical concepts for bulk energy storage. *Renew Sustain Energy Rev*. 2017;75:205-219. https://doi.org/10.1016/j.rser.2016.10.065
15. Desrues T, Ruer J, Marty P, Fourmigué JF. A thermal energy storage process for large scale electric applications. *Appl Therm Eng*. 2010;30(5):425-432. https://doi.org/10.1016/j.applthermaleng.2009.10.002
16. Wang L, Lin X, Chai L, Peng L, Yu D, Chen H. Cyclic transient behavior of the Joule–Brayton based pumped heat electricity storage: Modeling and analysis. *Renew Sustain Energy Rev*. 2019;111:523-534. https://doi.org/10.1016/j.rser.2019.03.056
17. Rundel PM, Daschner R, Binder S, Hornung A. Schüttgutspeicher zur Effizienzsteigerung von Druckluftspeicherkraftwerken. In: *13 Symposium Energieinnovation*. Graz, Austria; 2014:1-9.
18. Kasparek G. Insulations Materials (D6.5). In: VDI e. V., ed. *VDI Heat Atlas*, 2nd edn. Berlin, Heidelberg: Springer-Verlag; 2010:591-594.
19. Fraunholz C. Exergoökonomische Analyse von Strom-Wärme-Strom Speichersystemen angelehnt an adiabate Druckluftspeicher. Master Thesis, TU Darmstadt. 2016.
20. Krüger M, Schwarzenbart M, Zunft S. Verfahrensentwicklung für dezentrale adiabate Druckluftspeicherkraftwerke (Mini-CAES). In: *Thermodynamik-Kolloquium 2014*, Stuttgart, 2014. http://elib.dlr.de/90760/
21. Zunft S. Adiabatic CAES: The ADELE-ING project. In: *SCCER Heat & Electricity Storage Symposium*. Villingen, Switzerland; 2015.
22. Moser P. Status der Entwicklung des adiabaten Druckluftspeichers ADELE. In: *Halle: Leopoldina-Symposium*; 2014.
23. STEAG GmbH, EBSILON Professional, Process Simulation Software. Release 12.03.2016. http://www.steag-systemtechnologies.com
24. Dietrich A, Dammel F, Stephan P. Exergoeconomic analysis of a pumped heat electricity storage system with concrete thermal energy storage. *Int J Thermodyn*. 2016;19(1):43-51. https://doi.org/10.5541/ijot.5000156078
25. Ismail KAR, Stuginsky R Jr. A parametric study on possible fixed bed models for pcm and sensible heat storage. *Appl Therm Eng*. 1999;19(7):757_788. https://doi.org/10.1016/S1359-4311(98)00081-7
26. Hänchen M, Brückner S, Steinfeld A. High-temperature thermal storage using a packed bed of rocks – heat transfer analysis and experimental validation. *Appl Therm Eng*. 2011;31(10):1798-1806. https://doi.org/10.1016/j.applthermaleng.2010.10.034
27. Gil A, Medrano M, Martorell I, et al. State of the art on high temperature thermal energy storage for power generation. Part 1 - concepts, materials and modellization. *Renew Sustain Energy Rev*. 2010;14(1):31-55. https://doi.org/10.1016/j.rser.2009.07.035
28. Baehr HD, Kabelac S. *Thermodynamik Grundlagen und technische Anwendungen*, 15th edn. Berlin, Heidelberg: Springer-Lehrbuch, Springer Vieweg; 2012. https://doi.org/10.1007/978-3-642-24161-1.
29. Bejan A, Tsatsaronis G, Moran M. *Thermal Design and Optimization*. New York: Wiley-Interscience; 1996. https://www.wiley.com/en-us/Thermal+Design+and+Optimization-p-9780471584674.
30. Stephan P, Schaber K, Stephan K, Mayinger F. *Thermodynamik - Grundlagen und technische Anwendungen: Einstoffsysteme*, 17th Edition, Vol. 1 of Springer-Lehrbuch. Berlin, Heidelberg: Springer-Verlag; 2006. https://doi.org/10.1007/978-3-540-70814-8.
31. Tsatsaronis G. Thermoeconomic analysis and optimization of energy systems. *Progress Energy Combust Sci*. 1993;19(3):227-257. https://doi.org/10.1016/0360-1285(93)90016-8
32. Sciubba E, Wall G. A brief commented history of exergy from the beginnings to 2004. *Int J Thermodyn*. 2007;10(1):1-26. https://doi.org/10.5541/ijot.184
33. European Power Exchange, EPEX SPOT SE: Day-Ahead Auction. (Jan. 2017). https://www.epexspot.com/en/market-data/dayaheadauction
34. Deutscher Wetterdienst. Temperatur im Jahr 2016 nach Bundesländern, Statista - Statistik Portal (2017). https://de.statista.com/statistik/daten/studie/249928/umfrage/temperatur-im-jahr-nach-bundeslaendern/
35. Deutscher Wetterdienst, Temperatur im Jahr 2015 nach Bundesländern, Statista - Statistik Portal (2016). https://de.statista.com/statistik/daten/studie/249928/umfrage/temperatur-im-jahr-nach-bundeslaendern/
36. Turton R, Bailie RC, Whiting WB, Shaeiwitz JA, Bhattacharyya D. *Analysis, Synthesis, and Design of Chemical Processes*, 4th edn. Upper Saddle River: Pearson; 2013.
37. Towler GP, Sinnott RK. *Chemical Engineering Design: Principles, Practice, and Economics of Plant and Process Design*, 2nd edn. Boston, MA: Butterworth-Heinemann; 2013.
38. Balli O, Aras H, Hepbasli A. Exergoeconomic analysis of a combined heat and power (CHP) system. *Int J Energy Res*. 2008;32(4):273-289. https://doi.org/10.1002/er.1353
39. Bauzentrum Beckmann, *Costs of Basalt Chips*. (Mar. 2017). http://www.beckmann-bauzentrum.de/natursteinkeramik/zierkiessplittgeroell/zier-uwegesplitt.html
40. Chemical Engineering Plant Cost Index, Economic Indicators. *Chem Eng*. 2017; 3:92.
41. Ruer J. Installation and method for storing and returning electrical energy, US Patent US8627665 B2, Saipem S.A. (Jan. 2014). http://www.google.com/patents/US8627665
42. Ni F, Caram HS. Analysis of pumped heat electricity storage process using exponential matrix solutions. *Appl Therm*

Eng. 2015;84:34-44. https://doi.org/10.1016/j.applthermaleng.2015.02.046

43. Howes JS. Concept and development of a pumped heat electricity storage device. *Proc IEEE*. 2012;100(2):493-503. https://doi.org/10.1109/JPROC.2011.2174529
44. Howes JS, Macnaghten J. Energy storage apparatus and method for storing energy. European Patent EP2220343b1, Isentropic Ltd. (Jun. 2013). http://depatisnet.dpma.de/DepatisNet/depatisnet?action=bibdat&docid=EP000002220343B1
45. Howes JS, Macnaghten J. Apparatus for use as a heat pump, European Patent EP1872069 B1, Isentropic Ltd. (Nov. 2010). http://depatisnet.dpma.de/DepatisNet/depatisnet?action=bibdat&docid=EP000001872069B1
46. McTigue JD, White AJ, Markides CN. Parametric studies and optimisation of pumped thermal electricity storage. *Appl Energy*. 2015;137:800-811. https://doi.org/10.1016/j.apenergy.2014.08.039
47. White AJ, Parks G, Markides CN. Thermodynamic analysis of pumped thermal electricity storage. *Appl Therm Eng*. 2013;53(2):291-298. https://doi.org/10.1016/j.applthermaleng.2012.03.030
48. Morandin M, Henchoz S, Mercangöz M. *Thermo-Electrical Energy Storage: A New Type of Large Scale Energy Storage Based on Thermodynamic Cycles*. Geneva, Switzerland: World Engineers Convention; 2011.
49. Laughlin RB. Pumped thermal grid storage with heat exchange. *J Renew Sustain Energy*. 2017;9(4):044103. https://doi.org/10.1063/1.4994054
50. Strauß K. *Kraftwerkstechnik: zur Nutzung fossiler, nuklearer und regenerativer Energiequellen*, 6th edn. Berlin: VDI, Springer; 2013.
51. Tsotsas E. Heat and mass transfer in packed beds with fluid flow (M7). In: VDI e. V. ed. *VDI Heat Atlas*, 2nd edn. Berlin, Heidelberg: Springer-Verlag; 2010:1327-1342.

How to cite this article: Dietrich A, Dammel F, Stephan P. Exergoeconomic analysis of a pumped heat electricity storage system based on a Joule/Brayton cycle. *Energy Sci Eng*. 2021;9:645–660. https://doi.org/10.1002/ese3.850